[10] Schaechter, W., "Sounding Rocket Performance Approximations," Thiokol Chemical Corp., Ogden, Utah, presented at Unguided Rocket Ballistics Meteorology Conference, New Mexico State Univ., Las Cruces, N. Mex., Oct. 31–Nov. 2, 1967.
[11] Wilson, G. G., "Aeroballistic, Performance, Wind Effects and Payload Impact Dispersion and Flight Test Data for the Single-Stage Sandhawk Rocket System," SC-DR-291, July 1969, Sandia Labs., Albuquerque, N. Mex.

Numerical Analysis of Low-g Propellant Flow Problems

R. A. Madsen,* C. R. Easton,* and G. W. Burge†
McDonnell Douglas Astronautics Company, Western Division, Santa Monica, Calif.
AND
I. Catton‡
University of California, Los Angeles, Calif.

Introduction

The Marker- and Cell (MAC) numerical technique is capable of analyzing many of the low-g fluid flow and heating problems encountered with liquid propellant storage and supply systems. It can be used to calculate transient two-dimensional viscous flow and heating of fluid in a partially filled tank (which may contain baffles or an unusual initial liquid-vapor interface), for arbitrary prescribed initial and boundary conditions. Behavior of the liquid-vapor interface is calculated and interface breakup is permitted. An animated motion picture depicting the motion of the fluid, which is furnished as a portion of the computer output, is invaluable for rapidly assessing over-all features of calculated results. A detailed description of the MAC technique is presented in Ref. 1. Therefore only a brief description is given here.

The Navier Stokes and thermal-energy equations are cast in finite-difference form and solved explicitly as an initial value problem. A Poisson equation, derived from continuity, is solved for pressure by the Gauss-Seidel iterative method. For laminar flow with constant properties, the only approximation fundamental to the technique is that attributed to the finite-difference representation of the equations and the boundary conditions. Further approximations, such as linearizing equations or neglecting viscous effects are not necessary.

Typical meshes of computational cells are shown in Figs. 1–3. Velocities ($u_{i,j}$ and $u_{i+1,j}$, and $v_{i,j}$ and $v_{i,j+1}$) are defined on the sides of each cell. Pressure, temperature, and mass dilatation are defined at the center of each cell. At a rigid wall, either a free-slip velocity boundary condition (vanishing normal velocity component), or a no-slip velocity boundary condition (vanishing normal and tangential velocity components) can be applied. The free-slip condition, used herein, is appropriate when the thickness of the hydrodynamic boundary layer is much less than the width of a calculational cell. Boundary conditions at the liquid-vapor interface are selected to make the tangential shear stress vanish, to make the normal stress equal to the applied pressure, and to satisfy continuity in each surface cell. At an outlet cell, the outlet velocity history is prescribed and the required pressure gradient is determined from the momentum equation. Thermal boundary conditions are not of interest herein, because thermal effects were not considered in the examples presented.

Marker particles are set up as the numerical equivalent of neutrally buoyant particles used in laboratory flow-visualization experiments. They establish the location of the free surface and provide a visual display of fluid motion in computer-generated plots (Figs. 1–3). Marker particles are moved according to the local velocity at the end of each time step. The frames shown in Figs. 1–3 were printed directly from the microfilm output of a Stromberg Datagraphics SD-4060 microfilm recorder. After printing, outstanding features were overlayed on the prints.

Propellant Disturbances During Docking

A study was made of the propellant disturbances that could be expected in the LH_2 tank of the Saturn S-IVB stage

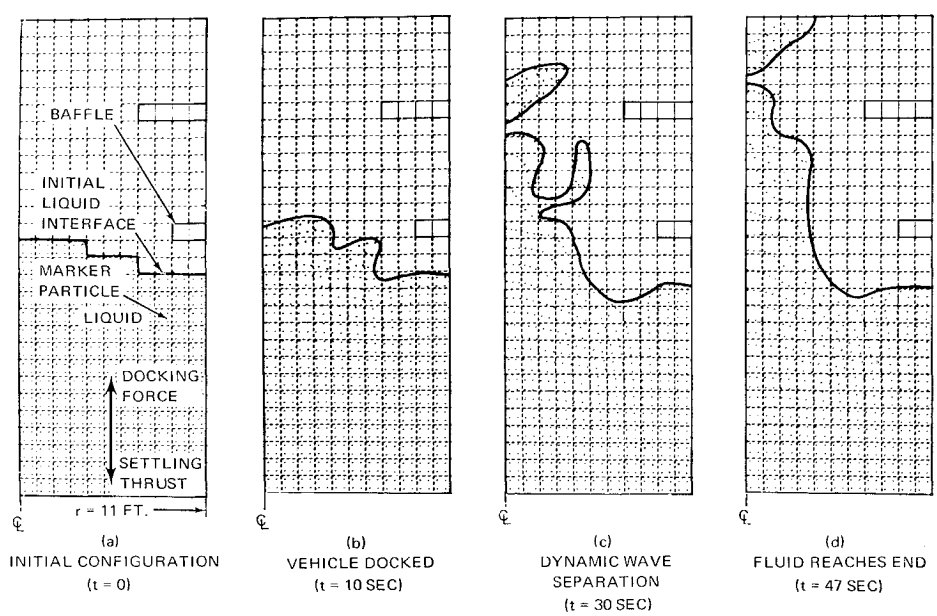

Fig. 1 Symmetric propellant unsettling.

Presented as Paper 69-567 at the AIAA 5th Propulsion Joint Specialist Conference, U.S. Air Force Academy, Colo., June 9–13, 1969; submitted July 11, 1969; revision received September 15, 1969. Portions of this work were sponsored by the NASA George C. Marshall Space Flight Center under Contract NAS 7-101.

* Senior Engineer Scientist, Advance Propulsion Department.
† Branch Chief, Liquid Propulsion Subsystems, Advance Propulsion Department. Member AIAA.
‡ Assistant Professor of Engineering. Member AIAA.

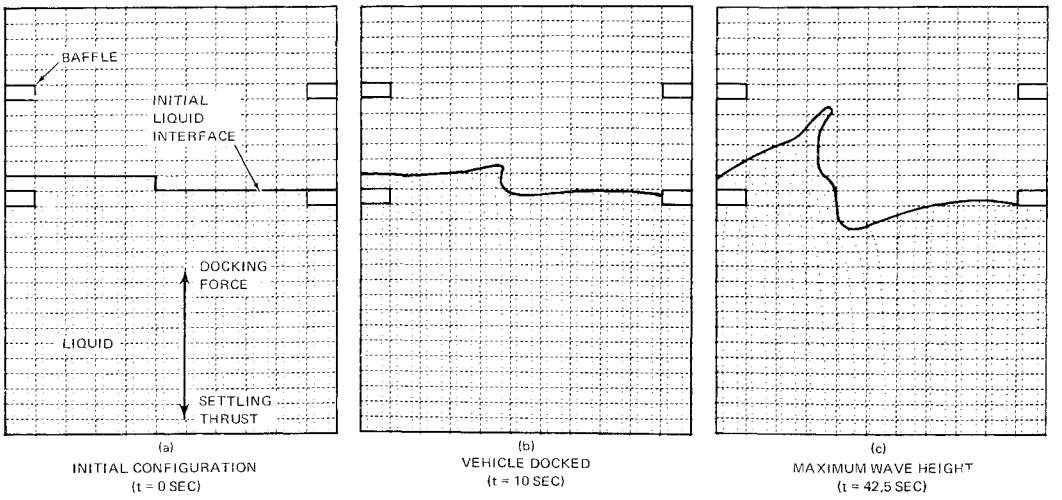

Fig. 2 Asymmetric propellant unsettling.

during and subsequent to the orbital docking maneuver of the AS-504D mission. In that mission, the Command and Service Module was docked with the Lunar Module (LM) which was attached to the forward dome of the S-IVB stage. The docking maneuver was performed prior to S-IVB restart, at which time a substantial amount of propellant remained in the S-IVB tanks. Prior to docking, the LH_2 was settled in the bottom of the tank. The impact of docking was in a direction to unsettle the LH_2. Because of the large quantity of propellant present in the S-IVB, a study of the propellant disturbance was pertinent to determine its effect on operating requirements for the attitude control system and the docking latch mechanism.

Under steady-state operation, a continuous settling acceleration of $4.5 \times 10^{-5} g_e$ is supplied to the S-IVB by the LH_2 continuous vent system. Various potential unsettling accelerations during docking were studied and it was estimated that the most severe axial impulse that could be expected was a 10-sec pulse of $1.45 \times 10^{-3} g_e$. This impulse, used in subsequent analyses, would be applied by the reaction control system of the spacecraft if the initial impact of docking was insufficient to latch the connector of the docking probe. Possible lateral accelerations were also estimated, but will not be discussed here. Disturbance of the LH_2 was calculated for initial liquid-vapor interface displacements in the forms of a symmetric slosh wave (Fig. 1) and an asymmetric slosh wave (Fig. 2).

Limitations of the particular MAC computer program utilized dictated that several assumptions be made. These assumptions are 1) the LH_2 tank was considered to have flat ends, 2) initial slosh waves were represented by discontinuous steps which matched calculational grid boundaries, 3) the asymmetric mode was studied in two-dimensional Cartesian coordinates, and 4) slip conditions were considered for the velocity at the walls of the tank. Effects from assumptions 1 and 4 should be of little consequence. Assumption 2 introduces an unrealistic effect in the initial propellant motion that takes a considerable period of time to dissipate. Assumption 3 renders results for that case qualitative in nature for a cylindrical tank.

In the cross-sectional views in Fig. 1, the tank centerline is located at the left edge of each frame; 1-ft^2 calculational grid was employed. A calculational time step of 0.5 sec was utilized and the total real-time duration covered was 53 sec. A computing time of 1 hr on a Univac 1108 computer was required.

In Fig. 1, considerable amplification of the initial two-step symmetrical wave had occurred by the time the unsettling impulse was removed and the steady-state settling acceleration became dominant again (Fig. 1b). At approximately 30 sec a spheroidal volume of liquid separated from the amplified wave (Fig. 1c). This liquid inundated the forward dome at 47 sec (Fig. 1d), after which resettling began. The calculations show that the major portion of the LH_2 remained seated in the tank and was not affected by the docking disturbance. Less than 1% of the total volume got above the upper slosh deflector.

For the two-dimensional asymmetric slosh wave problem in Fig. 2, a 1- × 2-ft calculation mesh and a computing time increment of 0.5 sec, were used. For a total real-time duration of 42.5 sec, the computer time was 1 hr.

Very little amplification of the wave had occurred by the time the unsettling impulse was removed and the steady-state settling acceleration became dominant again (Fig. 2b). Near peak amplitude was reached at 42.5 sec (Fig. 2c). Subsequent calculations indicated that the peak-wave amplification occurred at approximately 60 sec, at which time the tip of the wave shown in Fig. 2c reached the level of the upper slosh deflector. Again, the major portion of the LH_2 was unaffected by the docking disturbance. The portion that was affected was disturbed less than for the symmetric initial configuration.

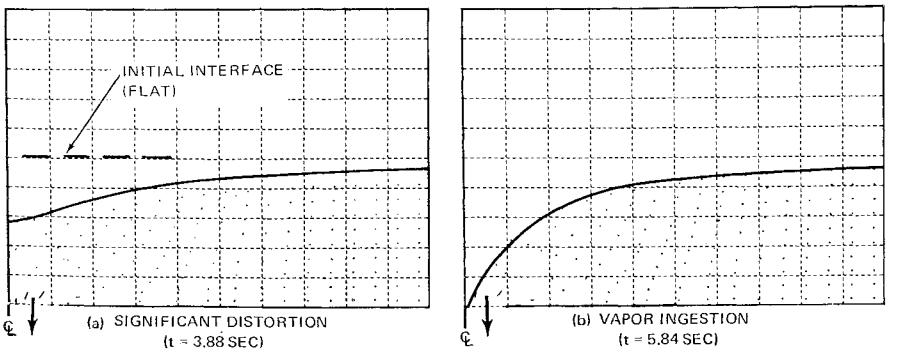

Fig. 3 Vapor ingestion during discharge.

Vapor Ingestion During Outflow

Prediction of the amount of liquid that remains in a tank when vapor ingestion occurs during discharge under low-g conditions is important for designing propellant transfer systems with minimum residual. Since surface displacements are large when vapor ingestion occurs, satisfactory prediction of liquid residual has not been possible with linearized, inviscid, free-surface-flow techniques. The MAC method utilizes the full Navier-Stokes equations, and as such has the capability for handling nonlinear effects.

Figure 3 shows some results for a 10-ft-diam tank, which had a 1-ft-diam drain in the center and was filled initially to a depth of 2.5 ft. A steady gravity level of $10^{-3}g_e$ and a flat initial liquid-vapor interface were considered. A 0.5-ft^2 calculation grid was utilized. The computing time increment was 0.04-sec, and the real-time duration was 6.0 sec. The computer time required was 6.5 min. The outflow velocity imposed as a boundary condition increased linearly from 0 to 5 fps in 1 sec and then remained constant. This outflow velocity was selected based on data from Ref. 2 as the value which will cause vapor ingestion to occur at a liquid-height/tank-diameter ratio (h/D) of 0.235. The outflow Froude number (Fr), as defined in Ref. 2, is 0.0781.

Calculated results in Fig. 3b show vapor ingestion initiating at 5.84 sec with $h/D = 0.23$, in close agreement with data of Ref. 2. Subsequent calculations made with larger initial liquid heights of 3.0 ft and 3.5 ft showed vapor ingestion at $h/D = 0.25$. Calculated h/D for a second, larger $Fr = 0.447$ compared similarly with data of Ref. 2.

References

[1] Welch, J. E. et al., "The MAC Method," LA-3425, March 1966, Los Alamos Scientific Lab., Los Alamos, N. Mex.

[2] Gluck, D. F. et al., "Distortion of a Free Surface During Tank Discharge," *Journal of Spacecraft and Rockets*, Vol. 3, No. 11, Nov. 1966, pp. 1691–1692.

Laminar Wall Jet with Blowing or Suction

Shoichiro Fukusako,* Masaru Kiya,† and Mikio Arie‡

Hokkaido University, Sapporo, Japan

Introduction

Although the effects of magnetic fields, suction or blowing, etc. on the boundary-layer flow along a solid surface have been extensively studied from the practical point of view of the boundary-layer control, very few studies are made concerning the flow properties and heat-transfer characteristics of a wall jet spreading over a permeable plane surface in otherwise stationary surroundings. The problem of laminar wall jet of this category was extensively studied by Fox and Steiger[1] by means of similar solutions. Their method of solution reduces to an eigenvalue problem and the distribution of suction and blowing velocities must be necessarily specified according to the eigenvalues. In fact, the normal velocity at the surface must be proportional to $x^{1/2(2\alpha-1)/(\alpha-1)}$, where x is a dimensionless coordinate along the surface and α is an eigenvalue. Although they state that an infinite number of similar solutions with each eigenvalue permit one to obtain a wide variety of distributions of normal velocity at the surface, we feel it worthwhile to construct a solution of more general applicability. In this Note suction and blowing velocities are assumed to be proportional to x^n, but, unlike Fox and Steiger's case, n may take any constant value. The solution is obtained as a perturbation from the laminar wall jet over an impermeable surface the solution of which was first obtained by Glauert.[2] Specific considerations are given to the case of wall jet over an isothermal permeable surface with uniform suction and blowing, the case of which is not included in Fox and Steiger's solution.

Received July 11, 1969; revision received September 8, 1969.

* Graduate Student, Department of Mechanical Engineering.

† Assistant Professor, Department of Mechanical Engineering.

‡ Professor, Department of Mechanical Engineering.

Analysis

The wall jet can be treated within the framework of the boundary-layer theory (Glauert[2]). In the following analysis, all velocities are referred to a characteristic velocity U and all lengths to ν/U. When the two-dimensional flow of an incompressible viscous fluid is steady and laminar, the boundary-layer equations become

$$\partial u/\partial x + \partial v/\partial y = 0 \tag{1}$$

$$u\partial u/\partial x + v\partial u/\partial y = \partial^2 u/\partial y^2 \tag{2}$$

$$u\partial T/\partial x + v\partial T/\partial y = (1/P_r)\,\partial^2 T/\partial y^2 \tag{3}$$

where x is the streamwise distance measured along the surface from an appropriate origin, y is the distance normal to the surface, u, v are the corresponding velocity components and T is the temperature. P_r is the Prandtl number. The isothermal surface temperature is T_w and the temperature of the surrounding fluid is T_∞. The boundary conditions are

$$y = 0: \quad u = 0,\ v = v_w x^n,\ \theta = 1 \tag{4}$$

$$y = \infty: \quad u = 0,\ \theta = 0 \tag{5}$$

where v_w is a constant and θ means $(T - T_\infty)/(T_w - T_\infty)$. $Uv_w x^n$ is the dimensional blowing or suction velocity; negative v_w implies suction and positive v_w blowing.

The continuity equation, Eq. (1), is automatically satisfied if the stream function ψ is introduced by the usual definition

$$u = \partial\psi/\partial y,\ v = -\partial\psi/\partial x$$

Here, we introduce the new variables

$$\xi = v_w x^{[(3/4)+n]},\ \eta = \tfrac{1}{2} y x^{-(3/4)}$$

and put the stream function and the temperature into the form

$$\psi(x,y) = 2x^{(1/4)}F(\xi,\eta)$$

$$\theta(x,y) = h_0(\eta) + \xi h_1(\eta) + \ldots \tag{6}$$

where

$$F(\xi,\eta) = f_0(\eta) + \xi f_1(\eta) + \ldots$$

The velocity components can now be expressed in terms of ξ and η

$$u = x^{-(1/2)}\partial F/\partial\eta \tag{7a}$$

$$v = -\frac{1}{2}x^{-(3/4)}\left[F - 3\eta\frac{\partial F}{\partial\eta} + (3+4n)\xi\frac{\partial F}{\partial\xi}\right] \tag{7b}$$

With Eqs. (6, 7a, and 7b), the momentum and energy equations can be written in terms of the new variables. Then, in each of the resulting equations, the terms are gathered according to the powers of ξ which multiply them. In this way, one obtains a set of ordinary differential equations for the functions f_0, h_0, f_1, h_1, . . .

$$f'''_0 + f_0 f''_0 + 2(f'_0)^2 = 0 \tag{8a}$$

$$h''_0 + P_r f_0 h'_0 = 0 \tag{8b}$$

$$f'''_1 + f_0 f''_1 + 4(n+1)f_1 f''_0 + (1-4n)f'_0 f'_1 = 0 \tag{8c}$$

$$h''_1 + P_r[f_0 h_1 + 4(n+1)f_1 h'_0 - (4n+3)f'_0 h_1] = 0 \tag{8d}$$